

Supporting Information

B-doped Core-Shell Fe@BC Nanozyme: Active Site Identification and Bacterial Inhibition

Xingxing Jiang,^{*a} Kang Liu,^b Qiang Li,^a Min Liu,^b Minghui Yang^{†a}, Xiang Chen^{†c}

^a College of Chemistry and Chemical Engineering, Central South University, Changsha, China, 410083

^b College of Physics and Electronics, Central South University, Changsha, China, 410083

^c Department of Dermatology, Xiangya Hospital, Central South University, Changsha, China, 410008

Corresponding author

*E-mail: M. Yang. yangminghui@csu.edu.cn

*E-mail: X. Chen. chenxck@yahoo.com

Experimental Section

Materials: Sodium Borohydride (NaBH_4), Terephthalic Acid (TA) and Propidium iodide (PI) were obtained from Sigma-Aldrich (St. Louis, MO, USA). SYTOTM 9 green fluorescent nucleic acid stain was purchased from ThermoFisher Scientific (Waltham, USA). Anhydrous ferrous chloride (FeCl_2) was purchased from Jiuding Chemical Technology Co., Ltd, (Shanghai, China). 3,3',5,5'-tetramethylbenzidine (TMB) was obtained from Aladdin (Shanghai, China). 2',7'-dichlorodihydrofluorescein diacetate (DCFH-DA), LB broth and LB broth with agar were purchased from Beyotime Biotechnology Co., Ltd (Shanghai, China). Dulbecco's Modified Eagle Medium, penicillin/streptomycin, and fetal bovine serum were obtained from ThermoFisher Scientific (Waltham, USA). Sodium hydroxide (NaOH) and Sodium acetate (CH_3COONa) were obtained from Hunan Chemical Reagent Co., Ltd, (Hunan, China). H_2O_2 (30%) was obtained from Xilong Chemical Co., Ltd, (Guangdong, China). Milli-Q water was used through the whole experiments and All chemicals were of analytical grade and used without further purification.

Characterizations: TEM images and EDX analyses were obtained using a JEOL-2100F (JEOL, Japan) electron microscope. UV-Vis was performed on a UV-Vis spectrophotometer (UV 2450, Shimadzu, Japan). Fourier transform infrared spectra (FT-IR) spectra were performed on Nicolet iS50 (ThermoFisher, USA). Scanning electron microscopy (SEM) images were recorded using a NOVA nano SEM230 (FEI, USA), Live/dead bacterial staining assay was imaged using the Olympus BX-51 optical system microscope (Olympus, Japan). XRD spectra were recorded by Ultima IV (Rigaku, Japan) and XPS spectra were performed using ESCACAB250 xi (ThermoFisher, USA). Raman spectra were recorded by InVia (Renishaw, England). Fluorescence spectrum and Ultraviolet spectrum were using an F-4600 Fluorescence spectrophotometer (HITACHI, Japan) and F-2450 UV Spectrophotometer (Shimadzu, Japan), respectively. The absorbance of CCK-8 was obtained by a microplate reader (Bio-Tek, USA). Pyrolysis was performed on a tubular furnace (OTX-200, Kejin, China). Electron paramagnet resonance (EPR) spectra were obtained by Bruker EMXmicro-6/1/P/L (Karlruhe, Germany).

Preparation of B-doped Fe@BC nanozyme: First, FeCl_2 solution (0.2 M, 20 mL) was placed in a three-necked round flask under stirring and N_2 purging and maintained at 4 °C for about 15 min. And then NaBH_4 solution (0.5 M, 10 mL) dissolved in 0.2 M NaOH solution was added into FeCl_2 aqueous solution dropwise and stirred at 4 °C under N_2 atmosphere for 30 min to obtain a black precipitate. The black precipitate was collected and washed by anhydrous ethanol and the collected precipitate covered by anhydrous ethanol (3 mL) was heat-treated at different temperatures (600 °C, 700 °C, 800 °C and 900 °C) under an argon atmosphere for 2 h. Finally, Fe@BC nanozymes were prepared. For the BC nanozyme without iron, NaBH_4 and anhydrous ethanol were heat-treated at 600 °C for 2 h according to the same protocol. For the Fe@BC-700-H, the same protocol was followed but annealed in mixed Ar/ H_2 gas.

Peroxidase-like Catalytic Activity of B-doped Fe@BC nanozyme: The color change of peroxidase-like Fe@BC-600 nanozymes toward TMB was photographed at room temperature after 10 min of co-incubation. The reaction solutions were carried out in 1 mL acetate buffer solution (0.2 M, pH = 3.5), the final concentrations of TMB, H_2O_2 , and Fe@BC nanozymes were 0.8 mM, 10 mM, and 10 $\mu\text{g mL}^{-1}$, respectively. All experiments were conducted at 37 °C in cuvette with a path length of 1.0 cm. Kinetic measurements were carried out by monitoring the change in absorbance at 652 nm. Spectra were recorded at 30 s intervals for a total of 10 min. Samples contained 10 $\mu\text{g mL}^{-1}$ Fe@BC-600 nanozymes, varied concentrations of TMB and H_2O_2 in 0.2 M acetate buffer (pH = 3.5), respectively. The apparent kinetic parameters were calculated using the Michaelis–Menten equation: $v = V_{\text{max}} \cdot [\text{S}] / (\text{K}_m + [\text{S}])$, where V_{max} represents the maximum reaction velocity, $[\text{S}]$ is the concentration of substrate, and K_m is the Michaelis constant. Parameters K_m and V_{max} were obtained from the double reciprocal

plot. For pH-dependent experiments, the enzyme-like activity of Fe@BC-600 was detected in the buffer solution with different pH ranging from 3 to 7, and for temperature-dependent experiments, measured in pH 3.5 acetate buffer under different temperatures ranging from 4 to 60 °C. For the catalytic activities of Fe@BC-600, Fe@BC-700, Fe@BC-800 and Fe@BC-900 in the presence of H₂O₂ were detected in pH 3.5 acetate buffer at 37 °C under the same conditions. For the peroxidase-like specific activity (U/mg), we tested the specific activity of Fe@BC-600 according to reported literature based on the equation: $b_{\text{nanozyme}} = V \cdot \Delta A / \epsilon l \cdot \Delta t$, where b_{nanozyme} is the nanozyme activity (U), V is the total volume of reaction solution (μL), ϵ is the molar absorption coefficient of the TMB substrate (39,000 M⁻¹ cm⁻¹ at 652 nm), l is the optical path length through reaction solution (cm), and $\Delta A / \Delta t$ is the initial rate (within 1 min) of the absorbance change (min⁻¹).¹ In details, 100 μL different concentrations of Fe@BC-600 (0.5, 10, 20, 30, 50 μg mL⁻¹) was added to catalyze TMB (0.8 mM TMB) by H₂O₂ (1 mM) in 0.2 M acetate buffer (pH= 3.5). By choosing 60 s (from 30 s to 90 s) as the initial rate period, the catalytic activity of the nanozyme expressed in units (U) was further calculated. When using different amounts of the Fe@BC-600 to trigger the TMB chromogenic reaction, it is observed that the activity measured is linearly increased with the amount of the nanozyme used. As a result, the specific activity of the Fe@BC-600 (U/mg) as a peroxidase mimic is determined.

Recyclability and dispersity of Fe@BC-600 nanozyme: To test the recyclability, the fresh and recovered 50 μg/mL⁻¹ Fe@BC-600 to catalyze TMB (0.8 mM TMB) by H₂O₂ (1 mM) in 0.2 M acetate buffer (pH= 3.5). The total absorbance was measured after 10 minutes reaction. The recovered Fe@BC-600 were separated from the reaction mixture by a magnet, and then washed with H₂O three times. The recycled Fe@BC-600 were mixed with a fresh reaction mixture again to remeasure and 10 runs were totally measured. For the dispersity, 1 mg mL⁻¹ Fe@BC-600 was dispersed in PBS (pH= 7.4) and its dispersity was analyzed by the Tyndall effect.

Catalase-like Catalytic Activity of B-doped Fe@BC nanozyme: The CAT-like activity of the Fe@BC-600 was determined by monitoring the change of fluorescence intensity of 2-hydroxy terephthalic acid (TAOH). H₂O₂ can decompose into •OH and react with terephthalic acid (TA) to generate TAOH, which displays an emission peak at 435 nm. H₂O₂ decomposes into H₂O and O₂, so TAOH could not generated in the presence of CAT (or CAT mimics). Based on these theories, we investigated the elimination of H₂O₂ by monitoring the fluorescence signal of TAOH. Phosphate buffer (PBS, 10 mM, pH 7.4) containing H₂O₂ (1 mM) and different concentrations of Fe@BC-600 (0, 20, 40, 60, 80, 100, 200 μg mL⁻¹) was vigorously vortexed and incubated at room temperature for 6 h in the dark. Finally, TA (1.875 mM) was added. After thorough mixing, the fluorescence of the mixture was measured. The CAT-like kinetics was determined by monitoring the decrease in absorbance of H₂O₂ at 240 nm. By varying the concentration of H₂O₂ (0-200 mM) in the presence of Fe@BC-600 (200 μg mL⁻¹) in the phosphate buffer (PBS, 10 mM, pH 7.4) under 37°C, and the corresponding Michaelis-Menten curves obtained, and then the kinetic parameters were calculated using the Michaelis–Menten equation: $v = V_{\text{max}} \cdot [S] / (K_m + [S])$.

Measurement of Hydroxyl Radical (•OH): The possibility of •OH generation from H₂O₂ catalyzed by the Fe@BC-600 was evaluated by monitoring the change of fluorescence intensity of 2-hydroxy terephthalic acid (TAOH) due to the oxidation of terephthalic acid (TA) in aqueous solution. •OH can reduce TA to form TAOH with the maximum FL peak at 435 nm. Five groups of solutions (H₂O₂, TA, Fe@BC-600, TA + Fe@BC-600 and TA + H₂O₂ + Fe@BC-600) were investigated. In detail, TA, H₂O₂ and Fe@BC-600 were 1.875 mM, 1 mM and 10 μg mL⁻¹ were mixed with 500 μL 0.2 M acetate buffer (pH= 3.5). The mixture was gently shaken and stored at room temperature for 12 h in the dark and then their corresponding fluorescence intensities were recorded. Meanwhile, we analyzed the effect of different concentrations of H₂O₂ on the •OH quantitation. In detail, TA (1.875 mM), H₂O₂ (0, 1, 2, 5, 10 mM) and Fe@BC-600 (50 μg mL⁻¹) were mixed thoroughly and then measured.

Generation of •OH determined by EPR spectra: The generation of •OH was evaluated by EPR spectrometer using DMPO spin-trapping adduct. Three groups were built: (1) 50 $\mu\text{g mL}^{-1}$ Fe@BC-600+40 mM DMPO+1 mM H_2O_2 (2) 50 $\mu\text{g mL}^{-1}$ Fe@BC-600+40 mM DMPO (3) 40 mM DMPO+1 mM H_2O_2 . All mixtures were dispersed in 0.2 M acetate buffer (pH= 3.5) and then measured.

Bacterial Culture and Antibacterial Activity Tests: *S. aureus* and *E. coli* were cultured in Luria–Bertani (LB) broth for 18 h to reach their logarithmic phase (10^9 CFU mL^{-1}). Then the prepared bacteria solution were continued to be incubated with Fe@BC-600 (100 $\mu\text{g mL}^{-1}$), H_2O_2 (100 μM), Fe@BC-600 + H_2O_2 and PBS (pH = 3.5) for 2 h, respectively. Afterward, these solutions were diluted 10^5 times and cultured on agar plates for 24 h at 37 °C for imaging with a camera. Likewise, the prepared *S. aureus* solution (10^7 CFU mL^{-1}) incubated with PBS (pH = 3.5), Fe@BC-600, Fe@BC-700, Fe@BC-800 and Fe@BC-900 in the presence of H_2O_2 for 2 h respectively. Afterward, these solutions were diluted 10^4 times and cultured on agar plates for 24 h at 37 °C for CFU enumeration and imaged with a camera.

SEM image of bacteria: Bacteria treated with Fe@BC-600 (10 $\mu\text{g mL}^{-1}$), H_2O_2 (100 μM), Fe@BC-600 + H_2O_2 and PBS (pH = 3.5) for 2 h, respectively, before harvesting at 4000 rpm s^{-1} for 5 min and washing with PBS (pH = 7) for 3 times. And then bacteria fixed in PBS containing 2.5% glutaraldehyde for 2 h at room temperature. The bacteria were further washed with PBS and dehydrated by a series of ethanol solutions (20%, 40%, 60%, 80% and 100%) for 10 min with each step. Finally, the bacteria were placed on the silicon wafer and dried at the room temperature, and then sputter coated with gold and imaged with SEM.

Measurement of Intracellular ROS: The oxidant-sensitive dye DCFH-DA was used to measure intracellular ROS levels. After reaching the logarithmic phase (10^7 CFU mL^{-1}), bacteria were collected by centrifugation and incubated with DCFH-DA (10 μM) for 30 min at 37 °C in the dark. The bacterial cells were then washed twice with PBS (pH = 7) and treated with Fe@BC-600 (100 $\mu\text{g mL}^{-1}$), H_2O_2 (100 μM), Fe@BC-600 + H_2O_2 and PBS (pH = 3.5) at 37 °C for 2 h. Intracellular ROS levels were measured using a Fluorescence spectrophotometer with excitation wavelength at 488 nm and emission at 525 nm.

Cytotoxicity assay: The cytotoxicity of Fe@BC-600 against HeLa cells was investigated by CCK-8 assay. Cells were cultured in DMEM culture medium with 10% fetal bovine serum and 1% penicillin-streptomycin at 37 °C in a humidified atmosphere of 5% CO_2 . 4×10^4 cells were cultured in 96-wells plate for 24 h, then different concentrations of Fe@BC-600 were added and further cultured for another 24 h. Finally, 100 μL CCK-8 solution was added and incubated for 2 h before measuring the absorbance value at 450 nm.

Live/Dead staining analysis: Bacteria incubated with Fe@BC-600 (100 $\mu\text{g mL}^{-1}$), H_2O_2 (100 μM), Fe@BC-600 + H_2O_2 and PBS (pH = 3.5) for 2 h, respectively. And then the bacteria solution was treated with 1 μL of 1 μM SYTO™ 9 and 10 μL of 1 mg mL^{-1} PI for 1 h. Next, the bacteria solution was further washed with PBS (pH = 7) 3 times and followed by imaging by a Fluorescence Microscope.

Computational methods: Our DFT calculations were performed by using the Vienna Ab initio Simulation Package (VASP).²⁻⁴ The projector augmented wave (PAW) method describes the effective potential between the ionic cores and electrons.⁵ We adopted the Perdew–Burke–Ernzerhof (PBE) functional with generalized gradient approximation (GGA) to calculate the exchange-correlation energy.⁶ The van der Waals (VDW) interactions were corrected using the D2 method of Grimme.⁷ The cutoff energy of plane wave was set to 400 eV, and the convergence criteria of energy and force were set as 10^{-4} eV/atom and 0.02 eV/Å, respectively. We built a nanoribbon to simulate the substrate. The reaction groups are embedded in the substrate with a vacuum gap of 15 Å in Y and Z directs. The positions of all the atoms in the supercell were fully relaxed during the geometry optimizations. A Monkhorst-Pack mesh with $2 \times 1 \times 1$ K-points was used for Brillouin zone integration. The Gibbs free energy of each elementary step was calculated as $\Delta G = \Delta E + \Delta ZPE - T \cdot \Delta S + n_e \cdot U$,^{8, 9} where ΔE is the

reaction energy calculated by the DFT. ΔZPE and ΔS are the changes in zero-point energies and entropy during the reaction, respectively. T is a constant (298.15 K). n_e and U are the number of electrons transferred and the applied electrode bias potential, respectively.

Supporting figures



Figure S1. Digital image of as-prepared Fe₂B nanoparticles.

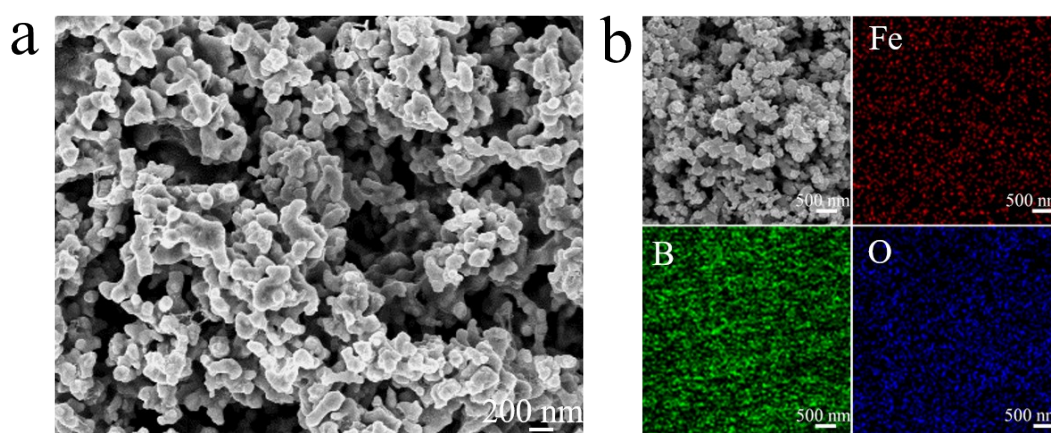


Figure S2. SEM images and EDX mapping of the Fe₂B particles.

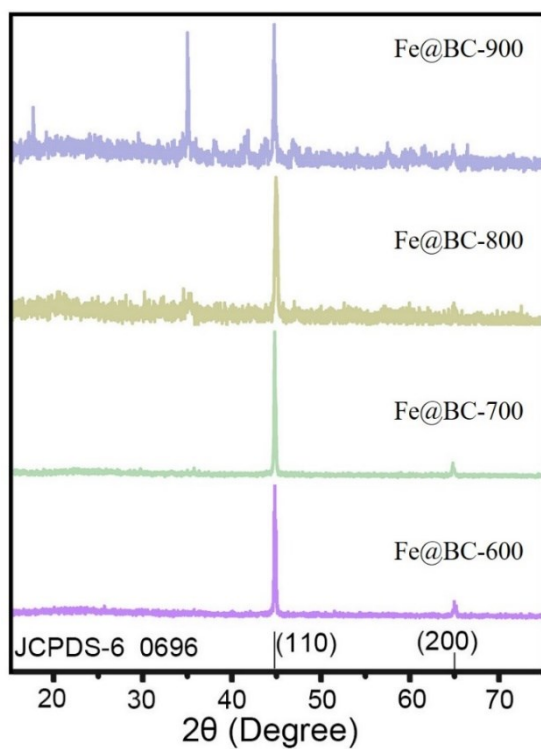


Figure S3. XRD analysis of various Fe@BC samples.

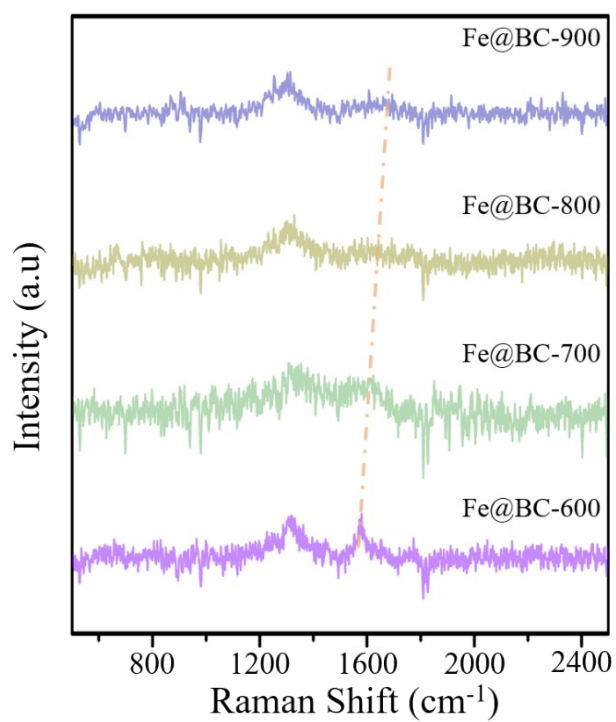


Figure S4. Raman spectra of various Fe@BC samples.

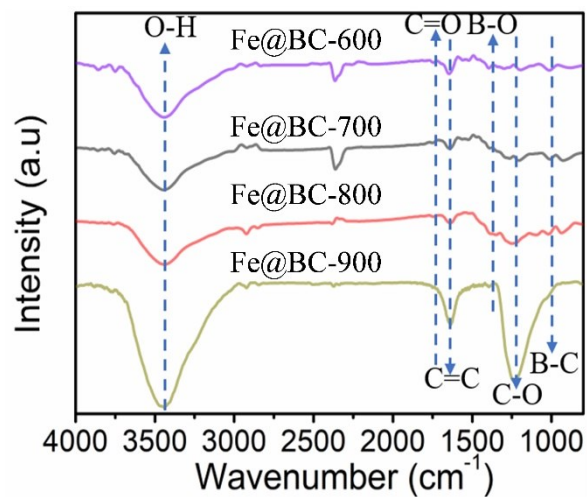


Figure S5. FTIR spectra of the Fe@BC-600, Fe@BC-700, Fe@BC-800 and Fe@BC-900, respectively

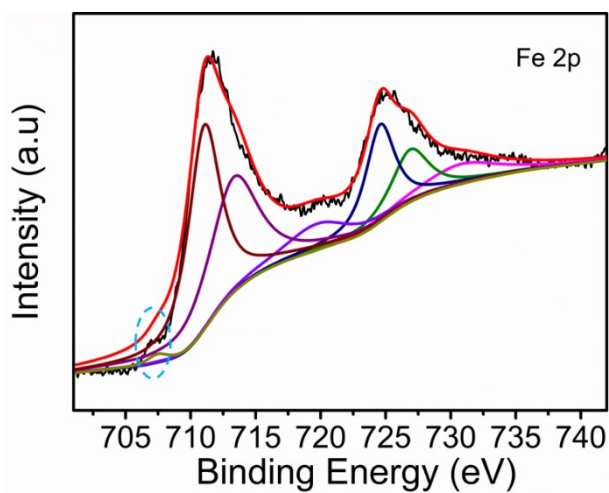


Figure S6. Fe 2p XPS spectra of the Fe@BC-600 sample.

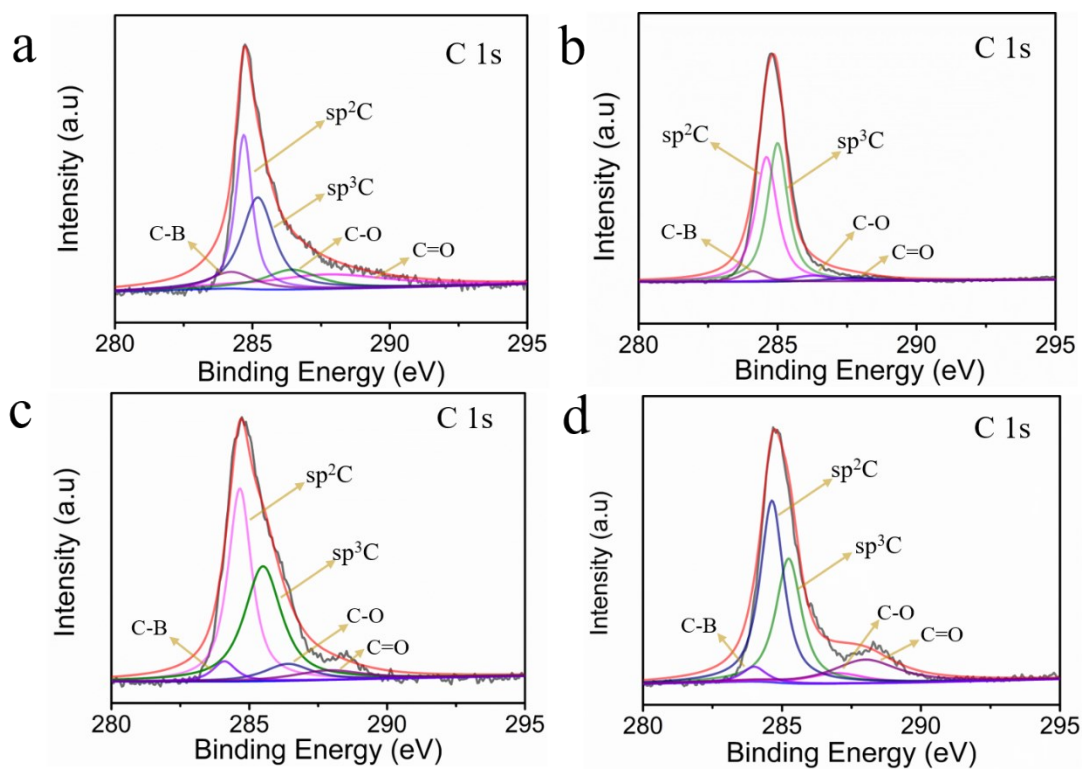


Figure S7. C 1s XPS spectra of a. Fe@BC-600, b. Fe@BC-700, c. Fe@BC-800 and d. Fe@BC-900.

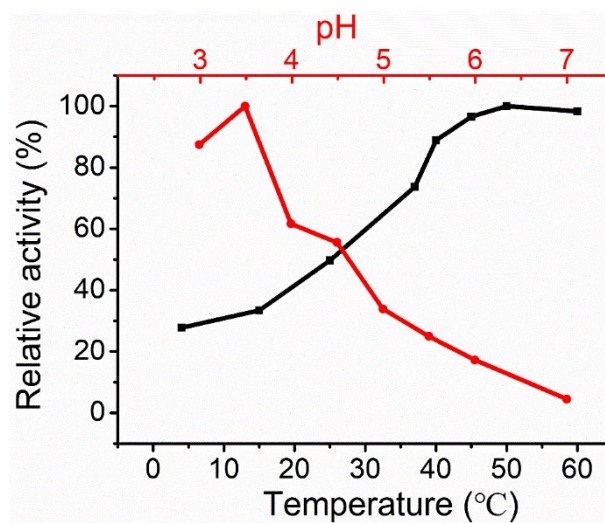


Figure S8. The peroxidase-like activities of Fe@BC-600 were dependent on temperature and pH.

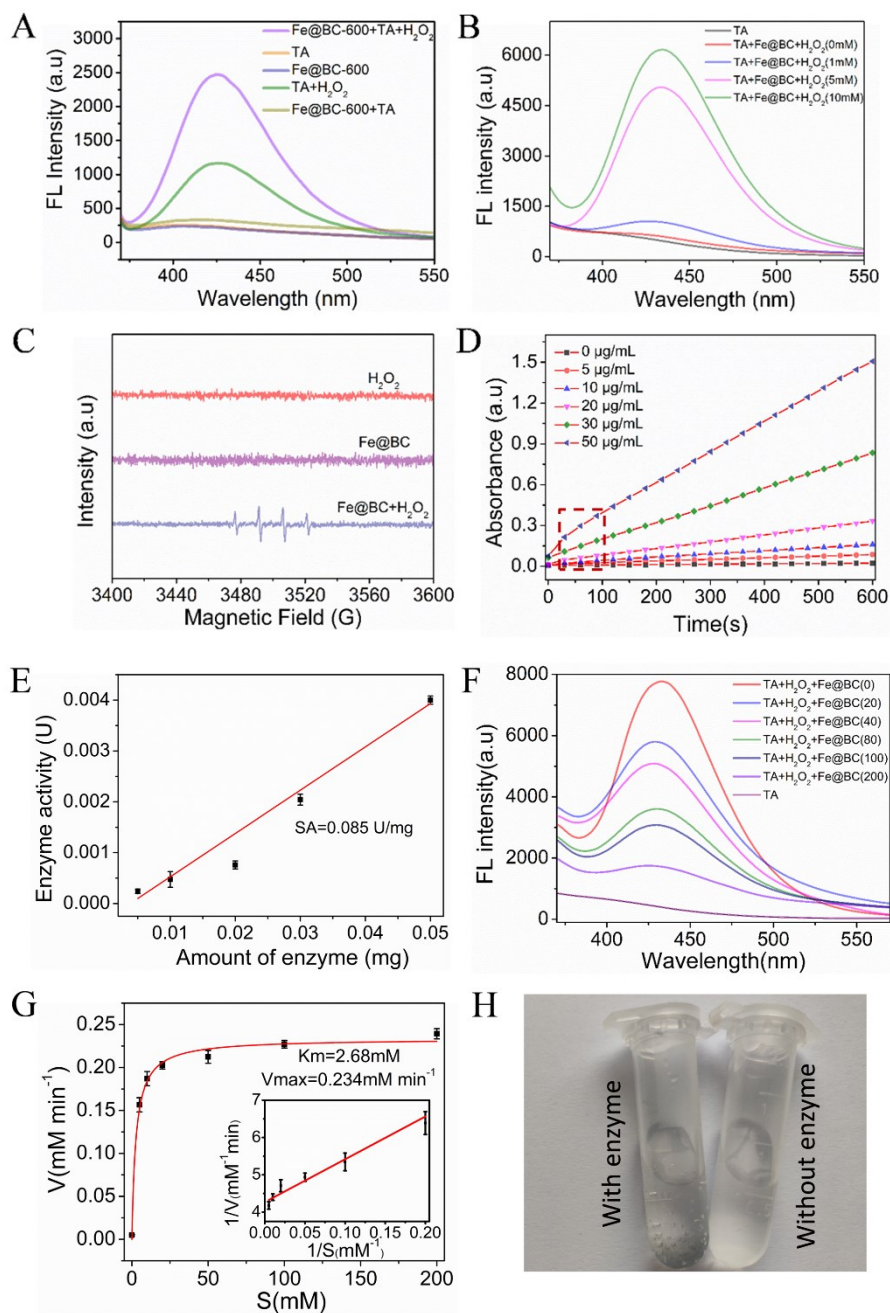


Figure S9. A). The 2-hydroxyterephthalic acid fluorescence obtained from different reaction systems to detect the $\cdot\text{OH}$ after 12 h carried out in acetate buffer (pH=3.5); B). The 2-hydroxyterephthalic acid fluorescence in presence of Fe@BC-600 ($50 \mu\text{g mL}^{-1}$) with different concentrations of H_2O_2 carried out in acetate buffer (pH=3.5); C). EPR spectra demonstrating $\cdot\text{OH}$ generation by H_2O_2 , Fe@BC-600, and Fe@BC-600 + H_2O_2 ; D). The absorbance-time curves of the TMB chromogenic reaction catalyzed by the Fe@BC-600; E). The relationship between the enzyme-like activity of the Fe@BC-600 and its amount; F). Fe@BC-600 also shows catalase-like activities, the intensity of 2-hydroxyterephthalic acid fluorescence peak was gradually reduced by the increased concentration of Fe@BC-600-induced decomposition of H_2O_2 (1 mM) in PBS (pH=7.4); G). CAT-like steady-state kinetic assay of Fe@BC-600; H). Bubbles were produced in the assist of Fe@BC-600, indicating the CAT-like activity.

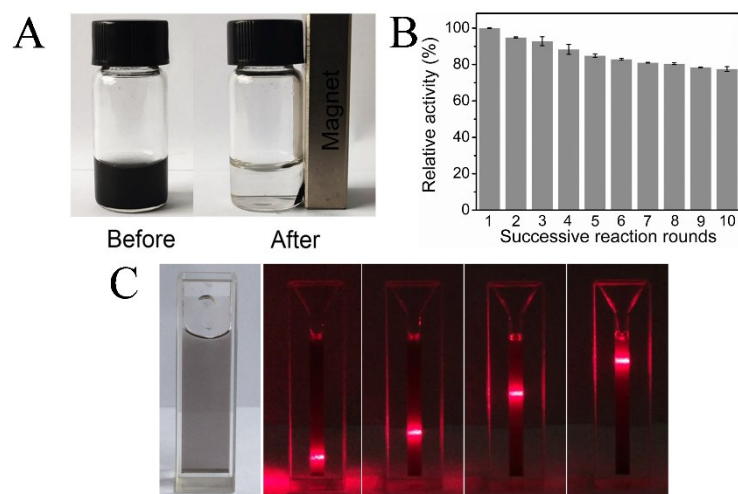


Figure S10. A). Photograph of PBS solution contains core-shell Fe@BC-600 nanozyme in the absence and presence of a magnet; B). The recyclability of nanozyme; C). The aqueous dispersibility of nanozyme analyzed by the Tyndall effect.

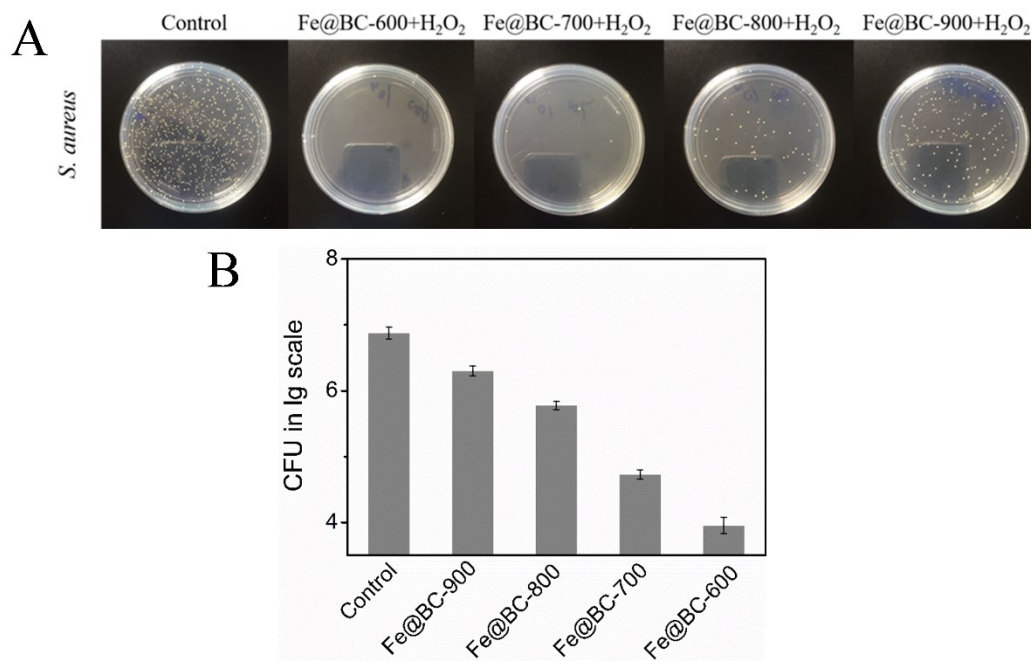


Figure S11. A). Photographs of *S. aureus* treated by various Fe@BC samples (100 $\mu\text{g mL}^{-1}$); B). CFU in lg scale of *S. aureus* after incubation with PBS (control), Fe@BC-600, Fe@BC-700, Fe@BC-800, Fe@BC-900 with H₂O₂, the used H₂O₂ concentration is 100 μM , Fe@BC-600 is 100 $\mu\text{g mL}^{-1}$.

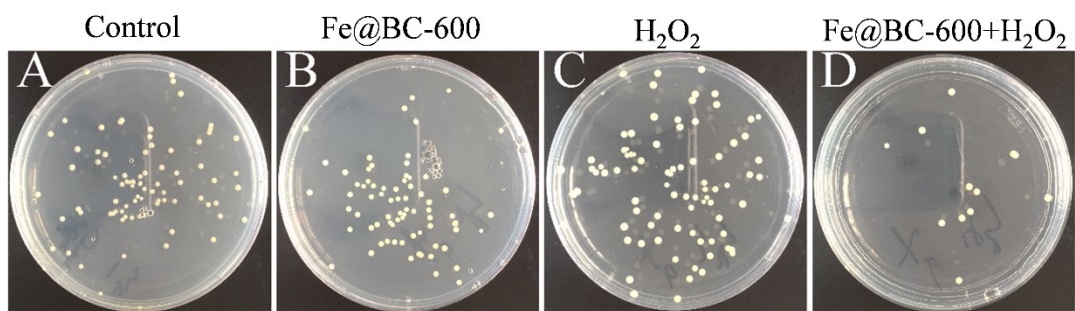


Figure S12. Photographs of *E. coli* treated by PBS (A), Fe@BC-600 (B), H₂O₂ (C) and Fe@BC-600+ H₂O₂ (D), the used H₂O₂ concentration is 100 μ M, Fe@BC-600 is 100 μ g mL⁻¹.

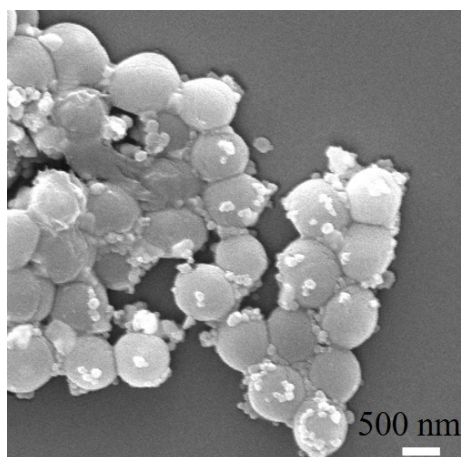


Figure S13. SEM images of *S. aureus* treated with Fe@BC-600.

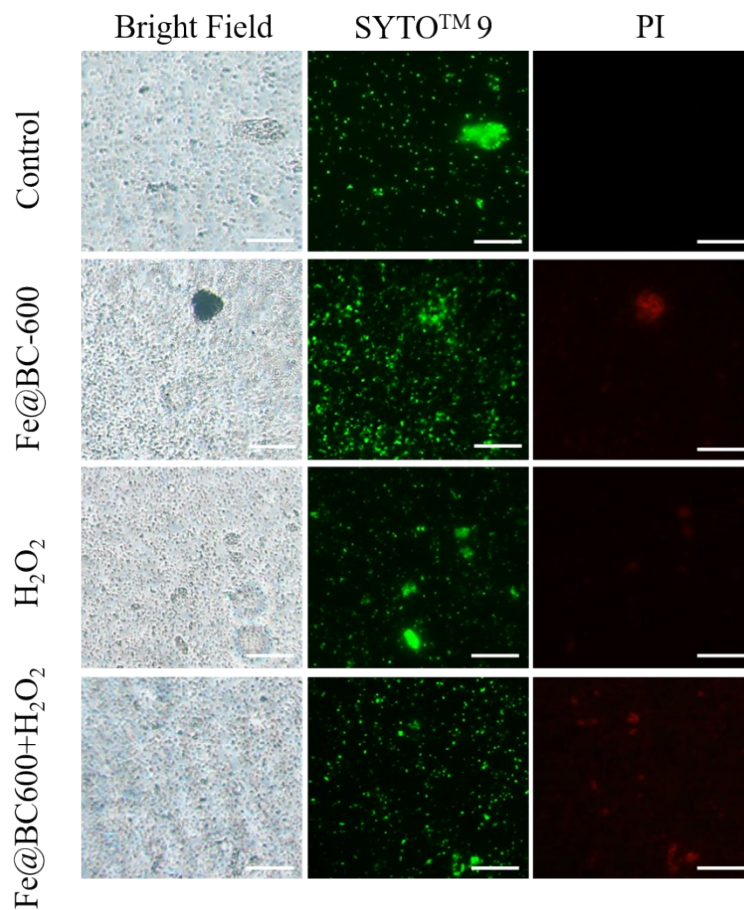


Figure S14. Fluorescence images for live/dead bacterial staining assay of *S. aureus* incubated with PBS (control), Fe@BC-600, H₂O₂ and Fe@BC-600+H₂O₂, respectively. The scale bar is 20 μ m.

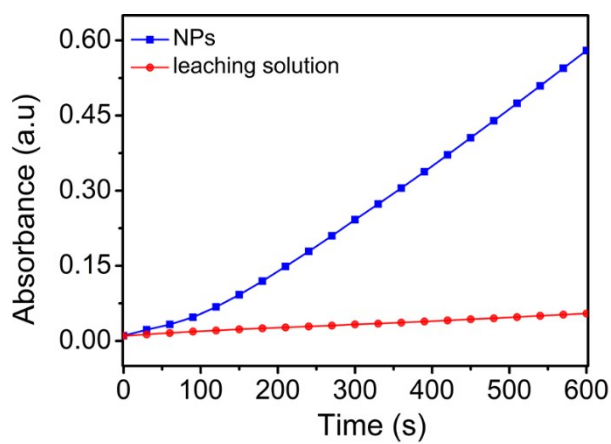


Figure S15. Time-dependent absorbance changes at 652 nm of TMB reaction solutions catalyzed by leaching solution and Fe@BC-600 nanozyme.

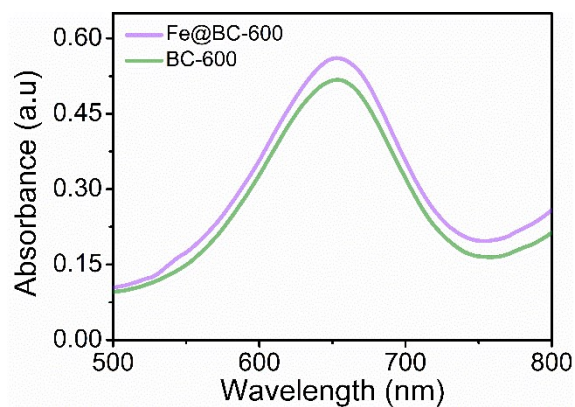


Figure S16. Peroxidase-like activity of Fe@BC-600 and BC-600.

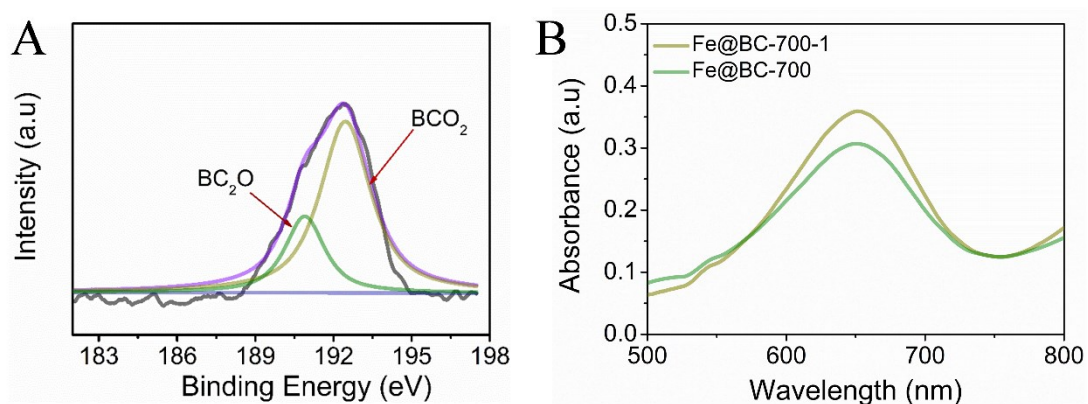


Figure S17. A) B 1s XPS spectra of Fe@BC-700-H. B) Peroxidase-like activity of Fe@BC-700-H and Fe@BC-700.

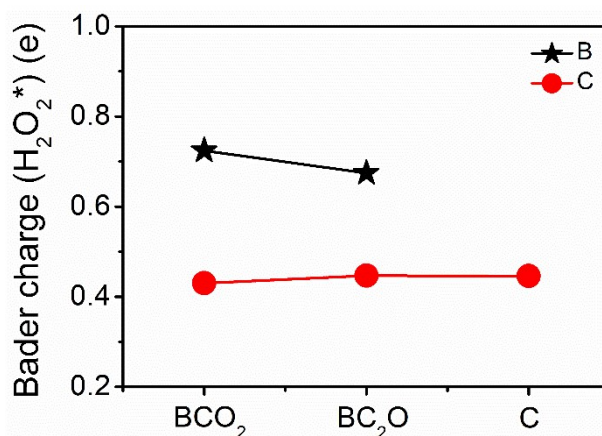


Figure S18. Bader charge analysis of absorbed H_2O_2^* on B and C sites of the B-doped structure.

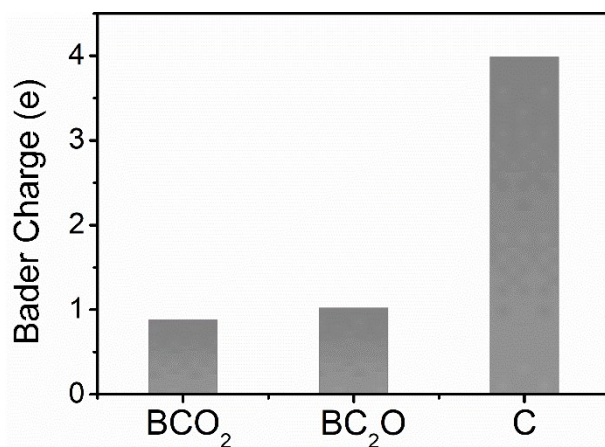


Figure S19. The analysis of charge number variation of B atom in the B-doped structures.

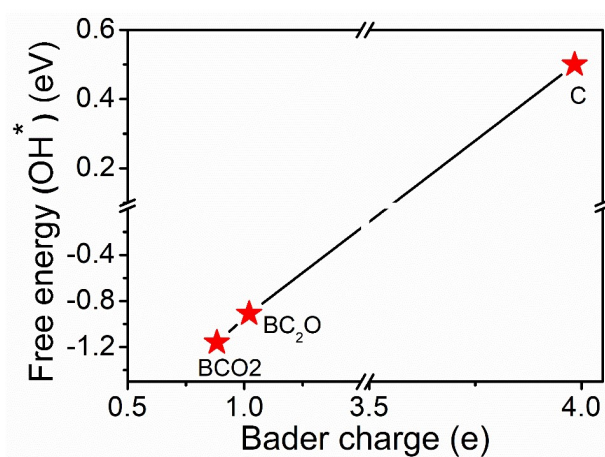


Figure S20. The free energy of OH* on C, BCO₂ and BC₂O structures.

Table S1. Elemental compositions of Fe and B in as-obtained Fe₂B particles

Material	Samples	Fe /wt%	B/wt%	Atomic ratio/%
Fe ₂ B	1	79.50	7.11	1.96
	2	78.60	7.17	
	3	79.30	7.15	
	4	70.60	7.66	
	5	70.90	7.72	
	6	71.40	7.84	

Table S2. The contents of sp²C of the corresponding samples based on XPS results

Samples	sp ² C	C _{total}	sp ² C/C _{total}
Fe@BC-600	4838.430	17292.130	0.280
Fe@BC-700	13576.000	33326.460	0.407
Fe@BC-800	7365.750	17334.890	0.424
Fe@BC-900	8995.540	21013.700	0.428

Table S3. Elemental compositions of Fe@BC samples detected by XPS

Samples	Fe/ at %	B/ at %	BCO ₂ / at %	BC ₂ O/ at %	C/ at %
Fe@BC-600	2.14	30.53	27.17	3.36	42.83
Fe@BC-700	6.99	17.00	11.05	5.95	34.24
Fe@BC-800	18.31	13.16	6.05	7.11	45.34
Fe@BC-900	15.04	12.61	5.92	6.69	47.03
Fe@BC-700-H	4.91	17.33	12.87	4.46	39.17

Note: The amounts of active sites (denoted as at %) of BCO₂ and BC₂O were calculated based on the at% of B, respectively.

Table S4. Kinetic parameters of the peroxidase-like activity of Fe@BC-600

Catalyst	Substrate	K _m /mM	V _{max} /10 ⁻⁸ MS ⁻¹
Fe@BC-600	TMB	1.00	8.74
	H ₂ O ₂	0.70	3.11

Table S5. Comparison of the kinetic parameters of Fe@BC-600 with other reported carbon nanozymes.

Enzymes	Substrate	Km (mM)	$V_{\max}(10^{-8}\text{MS}^{-1})$	References
GO-COOH	H ₂ O ₂	3.99	3.85	10
CQDs	H ₂ O ₂	26.77	30.61	11
C ₆₀ [C(COOH) ₂] ₂	H ₂ O ₂	24.58	4.01	12
MWCNT@rGNR	H ₂ O ₂	1.68	3.15	13
SWCNHs-COOH	H ₂ O ₂	49.8	2.07	14
HCNTs	H ₂ O ₂	41.42		15
GODs	H ₂ O ₂	1.17	1.24	16
Fe@BC-600	H ₂ O ₂	0.70	3.11	This work

REFERENCES

1. X. Niu, Q. Shi, W. Zhu, D. Liu, H. Tian, S. Fu, N. Cheng, S. Li, J. N. Smith, D. Du and Y. Lin, *Biosens Bioelectron*, 2019, **142**, 111495.
2. G. Kresse and J. Furthmüller, *Comp. Mater. Sci.*, 1996, **6**, 15-50.
3. G. Kresse and J. Furthmüller, *Phys. Rev. B: Condens. Matter Mater. Phys.*, 1996, **54**, 11169-11186.
4. G. Kresse and J. Hafner, *Phys. Rev. B: Condens. Matter Mater. Phys.*, 1994, **49**, 14251-14269.
5. P. E. Blochl, *Phys. Rev. B: Condens. Matter Mater. Phys.*, 1994, **50**, 17953-17979.
6. J. P. Perdew, J. A. Chevary, S. H. Vosko, K. A. Jackson, M. R. Pederson, D. J. Singh and C. Fiolhais, *Phys. Rev. B: Condens. Matter Mater. Phys.*, 1992, **46**, 6671-6687.
7. S. Grimme, *J. Comput. Chem.*, 2006, **27**, 1787-1799.
8. J. K. Nørskov, J. Rossmeisl, A. Logadottir, L. Lindqvist, J. R. Kitchin, T. Bligaard and H. Jonsson, *The Journal of Physical Chemistry B*, 2010, **108**, 17886-17892.
9. A. A. Peterson, F. Abild-Pedersen, F. Studt, J. Rossmeisl and J. K. Nørskov, *Energy Environ. Sci.*, 2010, **3**, 1311-1315.
10. Y. Song, K. Qu, C. Zhao, J. Ren and X. Qu, *Adv Mater*, 2010, **22**, 2206-2210.
11. W. B. Shi, Q. L. Wang, Y. J. Long, Z. L. Cheng, S. H. Chen, H. Z. Zheng and Y. M. Huang, *Chem Commun*, 2011, **47**, 6695-6697.

12. R. M. Li, M. M. Zhen, M. R. Guan, D. Q. Chen, G. Q. Zhang, J. C. Ge, P. Gong, C. R. Wang and C. Y. Shu, *Biosens Bioelectron*, 2013, **47**, 502-507.
13. J. Qian, X. W. Yang, Z. T. Yang, G. B. Zhu, H. P. Mao and K. Wang, *J Mater Chem B*, 2015, **3**, 1624-1632.
14. S. Y. Zhu, X. E. Zhao, J. M. You, G. B. Xu and H. Wang, *Analyst*, 2015, **140**, 6398-6403.
15. R. J. Cui, Z. D. Han and J. J. Zhu, *Chem-eur J*, 2011, **17**, 9377-9384.
16. H. J. Sun, A. D. Zhao, N. Gao, K. Li, J. S. Ren and X. G. Qu, *Angew Chem Int Edit*, 2015, **54**, 7176-7180.